Viscometry of Electron Fluids from Symmetry

Caleb Q. Cook and Andrew Lucas

Phys. Rev. Lett. **127**, 176603 — Published 22 October 2021

DOI: 10.1103/PhysRevLett.127.176603

Viscometry of electron fluids from symmetry

Caleb Q. Cook[1,*] and Andrew Lucas[2,3,†]

[1] *Department of Physics, Stanford University, Stanford CA 94305, USA*
[2] *Department of Physics, University of Colorado, Boulder CO 80309, USA*
[3] *Center for Theory of Quantum Matter, University of Colorado, Boulder CO 80309, USA*

When electrons flow as a viscous fluid in anisotropic metals, the reduced symmetry can lead to exotic viscosity tensors with many additional, non-standard components. We present a viscometry technique that can in principle measure the multiple dissipative viscosities allowed in isotropic and anisotropic fluids alike. By applying representation theory to exploit the intrinsic symmetry of the fluid, our viscometry is also exceptionally robust to both boundary complications and ballistic effects. We present the technique via the illustrative example of dihedral symmetry, relevant in this context as the point symmetry of 2D crystals. Finally, we propose a present-day realizable experiment for detecting, in a metal, a novel hydrodynamic phenomenon: the presence of rotational dissipation in an otherwise-isotropic fluid.

Introduction—Hydrodynamics models the transport of conserved quantities, such as charge or energy, over large length- and time-scales. In ultra-pure low-temperature metals, electronic momentum can also be approximately conserved, if the collisions that conserve momentum are much faster than those that relax it (e.g. off impurities or via umklapp) [1]. In these viscous electron fluids, hydrodynamic effects can give rise to exotic transport phenomena, such as decreasing resistance with increasing temperature (Gurzhi effect) [2] and superballistic constriction flow [3].

Theorized for many decades, electron hydrodynamics has in recent years garnered compelling experimental evidence [4–12]. The earliest discoveries of electron hydrodynamics took place in GaAs [4], monolayer graphene [5], and bilayer graphene [6]. At low (but non-zero) charge density, these are all isotropic Fermi liquids well-described by Galilean-invariant, textbook hydrodynamics [13]. For the electron fluid in graphene, the shear viscosity – the sole dominant viscosity in this isotropic Fermi liquid – has been both calculated [14, 15] and indirectly measured in experiment [6, 7, 11].

Metals are generically anisotropic, however, as the presence of a crystalline lattice explicitly breaks rotational symmetry. Indeed, experiments and *ab initio* calculations have recently suggested hydrodynamics might apply in less symmetric metals, e.g. WP_2 [16], $PtSn_4$ [17], MoP [18], WTe_2 [19]. In such cases, anisotropy leads to a number of novel phenomena [20], including rotational viscosity [21] and intrinsic Hall viscosity [22]. Such viscosities are inaccessible to current experiments, however, as existing methods (non-local resistances [23, 24], constriction conductances [3], AC phenomena [25], current imaging [10–12], channel flows [26], and heat transport [16, 27–29]) *(i)* are not robust to boundary and ballistic effects, and *(ii)* cannot distinguish all the symmetry-allowed viscosities that will generically appear.

Here, we present a multi-terminal device, robust to both boundary complications and ballistic effects, that can measure the multiple dissipative viscosity components allowed in isotropic *and* anisotropic fluids, all on a single sample. Our viscometry relies on the representation theory of point groups, from which we devise boundary conditions that isolate viscosities via symmetry-constrained heating. Our technique is also uniquely capable detecting a "smoking gun" signal of a novel hydrodynamic phenomenon: the isolated emergence of rotational viscosity $\eta_\circ$ in an "otherwise isotropic" fluid [21].

Strikingly, rotational viscosity $\eta_\circ$ gives viscous dissipation *even under rigid rotations of a fluid*, which is forbidden by angular momentum conservation in isotropic fluids, but generically allowed in anisotropic fluids. For hexagonal fluids in particular, $\eta_\circ$ emerges in a novel and isolated way [21], alongside only the standard, isotropic shear and bulk viscosities. Hexagonal electron fluids therefore provide a highly novel setting for finding $\eta_\circ$, with possible candidate materials including $PdCoO_2$ [30], $NaSn_2As_2$ [31], and ABA-trilayer graphene [32]. Finally, we argue that our viscometry proposed here is in fact the *only* feasible way of discovering $\eta_\circ$ in an electron fluid.

In what follows, we describe our viscometry via the illustrative example of 2D fluids of dihedral point symmetry. However, our approach extends naturally to fluids of higher dimension and/or differing point symmetry.

Dihedral hydrodynamics—The dihedral group D_{2M} is the $2M$-element group of symmetries of the regular M-gon. As an abstract group, D_{2M} is generated by its elements ρ, a $(2\pi/M)$-rotation about the M-gon center, and r, a reflection through a fixed axis containing the M-gon center, with $\rho r \rho = r$. We also take $\mathsf{D}_\infty = \mathsf{O}(2)$ to be the group of symmetries of the circle, which includes rotations of arbitrary angle. By the crystallographic restriction theorem [33], the paradigmatic 2D electron fluids are those of $M \in \{2, 3, 4, 6\}$ dihedral point symmetry.

In Newtonian fluids (appropriate for the linear response regime [1]), viscous stresses $\tau_{ij} = -\eta_{ijkl}\partial_k v_l$ arise linearly in response to velocity gradients $\partial_k v_l$, with proportionality given by the viscosity tensor η_{ijkl}. In the Supplemental Material (SM), we show that any D_{2M}-invariant viscosity tensor must take the form

$$\eta_{ijkl} = \begin{cases} \eta(\sigma^x_{ij}\sigma^x_{kl} + \sigma^z_{ij}\sigma^z_{jk}) + \zeta(\delta_{ij}\delta_{kl}), & M = \infty \\ \eta(\sigma^x_{ij}\sigma^x_{kl} + \sigma^z_{ij}\sigma^z_{jk}) + \zeta(\delta_{ij}\delta_{kl}) + \eta_\circ(\epsilon_{ij}\epsilon_{kl}), & M \in \{3\} \cup [5, \infty) \\ \eta_\times(\sigma^x_{ij}\sigma^x_{kl}) + \eta_+(\sigma^z_{ij}\sigma^z_{jk}) + \zeta(\delta_{ij}\delta_{kl}) + \eta_\circ(\epsilon_{ij}\epsilon_{kl}), & M = 4 \end{cases} \quad (1)$$

where ϵ is the Levi-Civita symbol and σ^a are Pauli matrices. We have excluded in Eq. (1) only the $M = 2$ viscosity tensor; in such D_4 fluids, one has eight allowed viscosities, not all of which are isolated by our viscometry due to the exceptionally-low symmetry of D_4. We therefore relegate discussion of this singular case to SM.

We emphasize that the presence of rotational viscosity $\eta_\circ$ in Eq. (1) does not rely on electrons or dihedral symmetry: it is universal to anisotropic fluids. The lack of rotational symmetry allows the stress tensor to have a nonvanishing antisymmetric component $\epsilon_{ij}\tau_{ij} \neq 0$, which in the hydrodynamics must couple to the strain tensor component $\epsilon_{ij}\partial_i v_j = \nabla \times \mathbf{v}$ of the same symmetry (i.e. the vorticity); this generic coupling is $\eta_\circ$. Fig. 1 illustrates the microscopic origin of $\eta_\circ$ in anisotropic electron fluids.

The remaining viscosities appearing in Eq. (1) can be understood as follows: bulk viscosity ζ [34] couples the trace of the stress tensor to the fluid expansion $\nabla \cdot \mathbf{v}$, plus viscosity η_+ couples the stress $(\tau_{xx} - \tau_{yy})$ along the axes of the crystal to the strain $(\partial_x v_x - \partial_y v_y)$, and cross viscosity $\eta_\times$ couples stress and strain at 45° to the crystal axes. Equating plus and cross viscosities $\eta_+, \eta_\times \to \eta$ in the D_8 tensor ($M = 4$) gives the D_{12} tensor ($M = 6$), and further taking $\eta_\circ \to 0$ in the D_{12} tensor gives the isotropic tensor ($M = \infty$). We therefore discuss dihedral viscosities without further loss of generality by henceforth assuming the D_8 case.

We now turn to the linearized (i.e. assuming Stokes flow [1, 13]) hydrodynamics. For D_8 fluids, the hydrodynamic equations are the following pair of approximate conservation laws:

$$\partial_t \rho = -\partial_i \left(\rho_0 v_i - D\partial_i \rho\right), \quad (2a)$$

$$\rho_0 \partial_t v_i = -c^2 \partial_i \rho - \rho_0 \Gamma v_i + \eta_{jikl}\partial_j \partial_k v_l, \quad (2b)$$

where ρ (ρ_0) is the (equilibrium) fluid density, c the electronic speed of sound, and Γ is the rate of momentum-relaxing collisions. Eq. (2a) describes the local conservation of density ρ, with an associated conserved current $J_i = \rho_0 v_i - D\partial_i \rho$. The current J_i has a convective contribution from the fluid momentum $\rho_0 v_i$ and a diffusive contribution $-D\partial_i \rho$, with D the incoherent diffusion constant [21, 35]. Eq. (2b) describes the approximate conservation of fluid momentum $\rho_0 v_i$ in the presence of viscous $-\partial_j \tau_{ji}$ and ohmic $-\rho_0 \Gamma v_i$ forces.

One may in principle append to Eq. (2) a third conservation law for energy. At $\rho_0 \neq 0$, this complication does not qualitatively modify the dynamics of homogeneous electron fluids [1]. At $\rho_0 = 0$ (e.g. the Dirac fluid of charge-neutral graphene), the energy density ϵ couples to velocity v_i in an analogous way to charge density ρ in Eq. (2). Due to this analogy we focus on the $\rho_0 \neq 0$ case, but our results are generalizable to Dirac fluids.

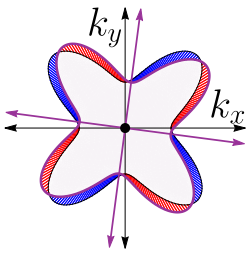

FIG. 1: Illustration of the origin of rotational viscosity in electron fluids. When an anisotropic Fermi surface (black) is rotated (dark purple), quasiparticle excitations (red/blue) are generated. In the hydrodynamic limit, such rigid rotations are opposed by a dissipative rotational viscosity $\eta_\circ$ [21]. Note that this Fermi surface has D_8 symmetry.

We now restrict to static flows $\partial_t = 0$, so that the left-hand-side of Eq. (2) vanishes. We can then automatically satisfy the resulting divergence-free condition on J_i 2a by writing the current in terms of a stream function: $J_i \equiv \rho_0 \epsilon_{ij}\partial_j \psi \implies v_i = (D/\rho_0)\partial_i \rho + \epsilon_{ij}\partial_j \psi$. Using this stream function ψ, we eliminate density ρ from the (static) momentum equation 2b and, neglecting terms of order $\eta D\partial^2 \psi \sim (\ell_{\rm ee}\partial)^2$, we find that the stream function satisfies the generalized biharmonic equation

$$\overline{\nabla}^4 \psi = \left(\frac{w}{\lambda}\right)^2 \overline{\nabla}^2 \psi + \delta\left[\left(\partial^2_{\overline{x}} - \partial^2_{\overline{y}}\right)^2 - \left(2\partial_{\overline{x}}\partial_{\overline{y}}\right)^2\right]\psi, \quad (3)$$

where we have introduced the parameters

$$\lambda = \sqrt{\frac{2\eta_\circ + \eta_+ + \eta_\times}{2\rho_0 \Gamma}}, \; \delta = \frac{\eta_+ - \eta_\times}{2\eta_\circ + \eta_+ + \eta_\times}, \quad (4)$$

and non-dimensionalized all lengths $(\overline{x}, \overline{y}) \equiv (x, y)/w$, $\overline{\nabla} \equiv \langle \partial_{\overline{x}}, \partial_{\overline{y}} \rangle$, using an assumed measurement lengthscale w (which will later characterize the size of our viscometer). Using an assumed solution ψ of the generalized biharmonic (3), we solve for $\partial_i \rho$ in Eq. (2b), which tells us that (away from $\rho_0 = 0$) the current $J_i \approx \rho_0 v_i$ is approximately coherent at this order [36]. Substituting this result into the stream function relation, we find that the fluid is approximately incompressible: $v_i \approx \epsilon_{ij}\partial_j \psi$.

The parameter λ (4) is known as the *Gurzhi length* and characterizes the length-scale past which momentum-relaxing effects begin to dominate viscous effects [1]. The dimensionless parameter δ (4) characterizes the degree of

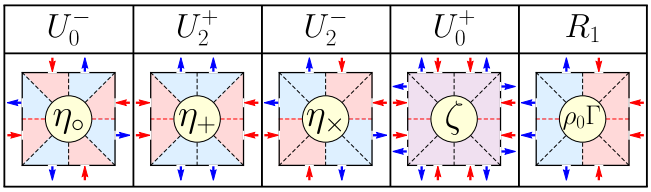

TABLE I: *First row*: The five irreducible representations of D_8. *Second row*: Current boundary conditions (blue/red arrows) of matching D_8-symmetry, indicated by colored wedges. Symmetry restricts heat (5) at the square center to *only* a single dissipative coefficient (yellow disk). Note that the representation U_0^+ requires more than 8 contacts in order to satisfy charge conservation.

square anisotropy in the fluid and must lie in the interval $\delta \in [-1, 1]$. The transformation $\delta \to -\delta$ corresponds to a rotation of the crystal coordinates by 45°, and $\delta = 0$ implies $\eta_+ = \eta_\times$ (no square anisotropy in the fluid).

Dihedral viscometry—Our dihedral viscometer is a square $(x, y) \in [-w/2, w/2]^2$, with current $J_i \approx \rho_0 v_i$ boundary conditions consisting of 8 contacts, each of width a, on its perimeter. Contacts are placed in pairs symmetrically about the midpoint of each edge, separated from each other by a tunable spacing d. A total current I_0 is either injected or drained at each contact, with the configuration of the viscometer determined by these choices. For concreteness, we take box function contacts [37], and no-slip $v_i = 0$ at the boundary away from contacts, in all numerical calculations (though our main results are unaffected by such details).

Our viscometry functions by exploiting the spatial symmetry of the dissipation generated in the fluid. The viscous dissipation is best understood via the irreducible symmetries of the D_8-invariant viscosity tensor, which we now outline; see SM for details.

Informally, a *group representation* [38] allows a group to act on a vector space, by assigning group elements to matrices in a way that is consistent with the underlying group multiplication. For finite groups and complex vector spaces, any such representation can be decomposed into a sum of elementary, "building-block" representations, known as *irreducible representations* (irreps). The dihedral group D_8 has five irreps: four 1-dimensional representations $U_{0,2}^{\pm}$ (the superscript denotes reflection parity, $U_k^{\pm}(r) = \pm 1$, and the subscript denotes rotation parity, $U_k^{\pm}(\rho) = \mathrm{i}^k$) and one 2-dimensional vector representation R_1 [21, 38]. These irreps label the five irreducible ways a mathematical object can self-consistently transform under reflection and 4-fold rotation. The irreps of D_8 and their realizations as current boundary conditions on a square are summarized in Table I.

Particularly relevant for viscometry is the 4-dimensional vector space $\mathcal{T}_2$ of rank-2 tensors, as the velocity strain tensor is an element of this space: $\partial_i v_j \in \mathcal{T}_2$. The viscosity tensor $\eta_{ij,kl} \equiv \eta_{ijkl}$ then acts linearly on $\mathcal{T}_2$ as a 4×4 matrix by index contraction. Since the viscosity tensor is D_8-invariant, Schur's lemma [38] implies that $\eta_{ij,kl}$ must act proportionally to the identity on each D_8-invariant subspace of $\mathcal{T}_2$. We illustrate this result by expressing the heat that is generated through viscous dissipation, $W_{\mathrm{visc}} = (\partial_i v_j)\eta_{ij,kl}(\partial_k v_l)$, as

$$\begin{aligned} W_{\mathrm{visc}} = \eta_\circ\,(\epsilon_{ij}\partial_i v_j)^2 + \eta_+(\sigma^z_{ij}\partial_i v_j)^2 \\ + \eta_\times(\sigma^x_{ij}\partial_i v_j)^2 + \zeta(\delta_{ij}\partial_i v_j)^2, \end{aligned} \tag{5}$$

where each term in Eq. (5) represents a projection of $\partial_i v_j$ into a given 1-dimensional D_8-invariant subspace of $\mathcal{T}_2$, corresponding to a 1-dimensional irrep of D_8.

Note that the total [39] heat $W = W_{\mathrm{visc}} + W_{\mathrm{ohm}}$ generated by the fluid flow also contains an ohmic contribution $W_{\mathrm{ohm}} = \rho_0 \Gamma v_i^2$. Even though $\rho_0\Gamma$ is not a component of the viscosity tensor, the fluid velocity v_i nevertheless transforms according to the remaining vector irrep R_1, conveniently completing our correspondence between D_8 irreps and dissipative coefficients in Table I.

Importantly, both the center of the square *and* its boundary are mapped to themselves under any D_8 symmetry transformation. Thus the center strain tensor $(\partial_i v_j)|_{\mathbf{r}=\mathbf{0}}$ and center velocity $v_i(\mathbf{0})$ must have the same D_8 symmetry as the square boundary. This implies that we can selectively isolate at the square center each of the 5 terms in the heat decomposition $W = W_{\mathrm{visc}} + W_{\mathrm{ohm}}$ by choosing boundary conditions corresponding to each of the 5 irreps of D_8.

The above considerations are summarized in Table I. A numerical demonstration of isolated $\eta_\circ$, η_+, and $\eta_\times$ heating is given in Fig. 2 (see SM for additional flow plots). In SM, we further show that our result does not fundamentally rely on hydrodynamics; across the *entire* ballistic-to-hydrodynamic crossover, our symmetry-based "viscometer" continues to isolate dissipation channels according to their symmetry.

The isolated center heat $W_{\mathbf{0}} = \eta_\alpha(\partial v_\alpha)^2_{\mathbf{0}}$ generated solely by the viscosity η_α sources a Poisson equation [5]

$$W = -\kappa\nabla^2 T \tag{6}$$

for temperature T, with κ the electronic thermal conductivity. If one is able to measure both the center temperature variation $(\nabla^2 T)_{\mathbf{0}}$ (e.g. by local thermometry [40, 41]) and center strain component $(\partial v_\alpha)_{\mathbf{0}}$ (e.g. by flow imaging [10–12]), then $\eta_\alpha = -\kappa(\nabla^2 T)_{\mathbf{0}}/(\partial v_\alpha)^2_{\mathbf{0}}$ can be determined. Alternatively, if one uses *only* local thermometry, one may still estimate $(\partial v_\alpha)_{\mathbf{0}}$ – and hence η_α – by mapping out heating patterns $W(x, y)$ via Eq. (6) and comparing against numerical simulations.

Another consistency check arises by varying the viscometer geometry. Numerically solving Eq. (3) for varying contact spacing d, we show in Fig. 3 how the anisotropy δ can be determined experimentally. The center heat $W_{\mathbf{0}}(d)$ (as a function of contact spacing d) varies

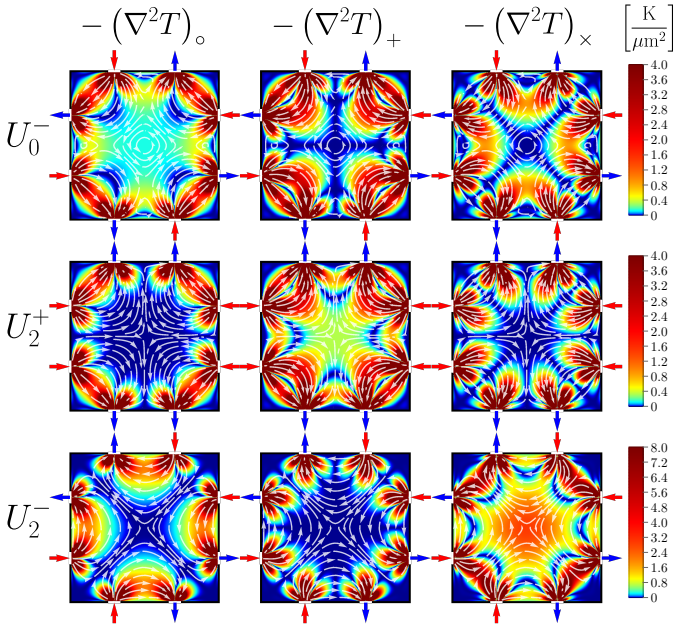

FIG. 2: Flows numerically solving Eq. (3) in our viscometer with $w = 1\ \mu$m, $I_0 = 100\ \mu$A, $d/w = 0.41$, $a/w = 0.05$, $\delta = 0$, and $\lambda/w = \infty$. Rows specify D_8-irreducible boundary conditions, and columns the temperature variation $-(\nabla^2 T)_\alpha$ sourced solely by η_α-dissipation. Symmetry restricts center heating to only the diagonal plots. In giving an order-of-magnitude estimate for the scale of heating, we have taken relevant physical parameters from hydrodynamic electrons in monolayer graphene [6, 7]; see SM. Temperature variations of this magnitude are detectable with existing local thermometers [40, 41].

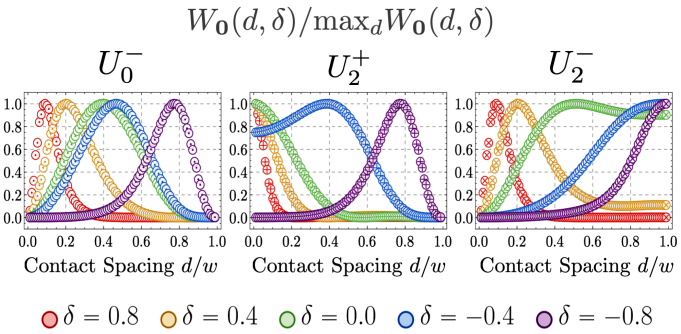

FIG. 3: Viscometer center heat $W_{\mathbf{0}}$, numerically determined from Eq. (3), as a function of boundary condition irrep., contact spacing d, and anisotropy δ, for $a/w = 0.01$ and $\lambda/w = \infty$. Each curve is normalized by its max value. The uniqueness of these curves should allow for experimental determination of δ. Although momentum-relaxation is neglected in these $\lambda/w = \infty$ plots, we find that the shape of these curves, and hence their utility in determining δ, is extremely insensitive to decreasing λ (increasing Γ); see SM.

uniquely with anisotropy δ, allowing for computation of the latter. In fact, we show in SM how δ may be determined from as few as 2 contact spacings and 2 boundary configurations, for 4 total center heat measurements.

Finally, in SM we discuss how our viscometry compares against more conventional Poiseuille, channel flow methods, particularly in the D_4 case [26] where there is insufficient symmetry to isolate all viscosities via boundary conditions, as above.

Conclusions—Even if the above procedure cannot be carried out in full, one may nevertheless *detect* rotational viscosity $\eta_\circ$ by simply observing center heat in the U_0^- configuration. U_0^--symmetry precludes any center heat that might arise from another viscosity component, ohmic effects, incoherent currents, or even ballistic scattering (in addition to being highly suppressed in the viscous limit, ballistic center heat also has easily distinguishable scaling with viscometer size w; see SM). We therefore anticipate that our viscometry can enable the discovery of $\eta_\circ$ in the near future.

We further claim that (in contrast to other dihedral viscosities) there is no feasible way to detect $\eta_\circ$ beyond the symmetry-based technique proposed here. Expanding the hexagonal viscosity tensor (1) in Eq. (2b), one in fact obtains the *isotropic* momentum equation, but with replacements $\{\eta, \zeta\} \to \{\eta + \eta_\circ, \zeta - \eta_\circ\}$. This implies that *rotational viscosity does not modify bulk flow patterns*. Although exotic no-stress boundary conditions can in principle generate weakly $\eta_\circ$-dependent flows, the incomplete understanding of viscous electron boundary conditions makes it is unclear how such an experiment could be robustly carried out.

Indeed, there has been much discussion concerning the proper boundary conditions (e.g. no-slip, no-stress, generalized Robin) for viscous electron flow [42–44]. Because our viscometer relies on symmetry, it conveniently sidesteps any such boundary complication, so long as the boundaries are symmetrically complicated. For example, although we assumed no-slip $v_i = 0$ boundary conditions in the preceeding numerics, if no-stress or generalized Robin boundary conditions are instead required, the numerical values in Figs. 2 and 3 will change but the irrep decomposition of the rank-2 tensor space $\mathcal{T}_2$ will continue to guarantee isolated center heating.

We emphasize that our viscometry extends to more general fluids. For fluids of point group symmetry G, one constructs a device with G-irreducible boundary conditions. Then the viscous heat generated at a G-invariant point (i.e. mapped to itself under the action of G) can be selectively restricted to each irreducible comnponent of the viscosity tensor, as above. Our viscometery therefore also generalizes to higher dimensions, although measuring local heating at the center of a 3D sample may be more challenging.

Finally, for fluids with broken inversion and time-reversal symmetries, additional non-dissipative tensors [45–47] may appear in η_{ijkl} (1). We compute these lower-symmetry tensors in SM, matching those found in recent work on anisotropic Hall viscosities [45]. We expect our viscometry to *partially* extend to such fluids, since tailored boundary conditions will be able to similarly isolate in experiment the effects of symmetry-constrained Hall viscosisties. However, while neither Hall viscosity nor $\eta_\circ$ modify the form of the Navier-Stokes equations, the Hall viscosity is, moreover, *non-dissipative*. Thus, for our viscometry to prove fully applicable to Hall viscosities, an experimental signature beyond heating must first be identified.

We thank Irving Dai and David Goldhaber-Gordon for helpful discussions. CQC was supported by NSF Grant No. DMR2000987. AL was supported by a Research Fellowship from the Alfred P. Sloan Foundation through Grant FG-2020-13795, and by the Gordon and Betty Moore Foundation's EPiQS Initiative via Grant GBMF10279.

* calebqcook@gmail.com
† andrew.j.lucas@colorado.edu

[1] A. Lucas and K. C. Fong. "Hydrodynamics of electrons in graphene", arXiv:1710.08425.
[2] R. N. Gurzhi. "Minimum of resistance in impurity-free conductors", *Journal of Experimental and Theoretical Physics* **17** 521 (1963).
[3] H. Guo, E. Ilseven, G. Falkovich, and L. Levitov. "Higher-than-ballistic conduction of viscous electron flows", *Proceedings of the National Academy of Sciences* **114** 3068 (2017), arXiv:1607.07269.
[4] M. J. M. de Jong and L. W. Molenkamp. "Hydrodynamic electron flow in high-mobility wires", *Physical Review* **B51** 11389 (1995), arXiv:cond-mat/9411067.
[5] J. Crossno *et al.* "Observation of the Dirac fluid and the breakdown of the Wiedemann-Franz law in graphene", *Science* **351** 1058 (2016), arXiv:1509.04713.
[6] D. A. Bandurin *et al.* "Negative local resistance due to viscous electron backflow in graphene", *Science* **351** 1055 (2016), arXiv:1509.04165.
[7] R. Krishna Kumar *et al.* "Superballistic flow of viscous electron fluid through graphene constrictions", *Nature Physics* **13** (2017), arXiv:1703.06672.
[8] D. A. Bandurin, A. V. Shytov, L. S. Levitov, R. K. Kumar, A. I. Berdyugin, M. Ben Shalom, I. V. Grigorieva, A. K. Geim, and G. Falkovich. "Fluidity onset in graphene", *Nature Communications* **9** 4533 (2018), arXiv:1806.03231.
[9] E. V. Levinson, G. M. Gusev, A. D. Levin, E. V. Levinson, and A. K. Bakarov. "Viscous electron flow in mesoscopic two-dimensional electron gas", *AIP Advances* **8** 025318 (2018), arXiv:1802.09619.
[10] J. A. Sulpizio *et al.* "Visualizing Poiseuille flow of hydrodynamic electrons", *Nature* **576** 75 (2019), arXiv:1905.11662.
[11] M. J. H. Ku *et al.* "Imaging viscous flow of the Dirac fluid in graphene", *Nature* **583** 537 (2020), arXiv:1905.10791.
[12] A. Jenkins, S. Baumann, H. Zhou, S. A. Meynell, D. Yang, K. Watanabe, T. Taniguchi, A. Lucas, A. F. Young, and A. C. Blesynski Jayich. "Imaging the breakdown of ohmic transport in graphene", arXiv:2002.05065.
[13] L.D. Landau and E.M. Lifshitz. *Fluid Mechanics* (Butterworth Heinemann, 2nd ed., 1987).
[14] A. Principi, G. Vignale, M. Carrega, and M. Polini. "Bulk and shear viscosities of the 2D electron liquid in a doped graphene sheet", *Physical Review* **B93** 125410 (2016), arXiv:1506.06030.
[15] B. N. Narozhny and M. Schütt. "Magnetohydrodynamics in graphene: shear and Hall viscosities", *Physical Review* **B93** (2016).
[16] J. Gooth *et al.* "Thermal and electrical signatures of a hydrodynamic electron fluid in tungsten diphosphide", *Nature Communications* **9** 1 (2018).
[17] C. Fu *et al.* "Thermoelectric signatures of the electron-phonon fluid in PtSn4", arXiv:1802.09468.
[18] N. Kumar *et al.* "Extremely high conductivity observed in the triple point topological metal MoP", *Nature Communications* **10** 2475 (2019).
[19] U. Vool *et al.* "Imaging phonon-mediated hydrodynamic flow in WTe2 with cryogenic quantum magnetometry", arXiv:2009.04477.
[20] G. Varnavides, A. Jermyn, P. Anikeeva, C. Felser, and P. Narang. "Electron hydrodynamics in anisotropic materials", *Nature Communications* **11** 1 (2020), arXiv:2002.08976.
[21] C. Cook and A. Lucas. "Electron hydrodynamics with a polygonal Fermi surface", *Physical Review B* **99** 23 (2019), arXiv:1903.05652.
[22] R. Toshio, K .Takasan, and N. Kawakami. "Anomalous hydrodynamic transport in interacting noncentrosymmetric metals", *Physical Review Research* **2** 3 (2020).
[23] I. Torre, A. Tomadin, A. K. Geim, and M. Polini. "Non-local transport and the hydrodynamic shear viscosity in graphene", *Physical Review* **B92** 165433 (2016), arXiv:1508.00363.
[24] L. Levitov and G. Falkovich. "Electron viscosity, current vortices and negative nonlocal resistance in graphene", *Nature Physics* **12** 672 (2016), arXiv:1508.00836.
[25] A. Tomadin, G. Vignale, and M. Polini. "Corbino disk viscometer for 2D quantum electron liquids", *Physical Review Letters* **113** 23 (2014), arXiv:1401.0938.
[26] J. M. Link, B. N. Narozhny, E. I. Kiselev, and J. Schmalian. "Out-of-bounds hydrodynamics in anisotropic Dirac fluids", *Physical Review Letters* **120** 196801 (2018), arXiv:1708.02759.
[27] A. Principi and G. Vignale. "Violation of the Wiedemann-Franz law in hydrodynamic electron liquids", *Physical Review Letters* **115** 056603 (2015).
[28] A. Jaoui *et. al.* "Departure from the WiedemannFranz law in WP_2 driven by mismatch in T-square resistivity prefactors", *npj Quant Mater* **3** 64 (2018).
[29] A. Jaoui, B. Fauqu, and K. Behnia. "Thermal resistivity and hydrodynamics of the degenerate electron fluid in antimony", *Nature Communications* **12** 195 (2021).
[30] P. J. W. Moll, P. Kushwaha, N. Nandi, B. Schmidt, and A. P. Mackenzie. "Evidence for hydrodynamic electron flow in $PdCoO_2$", *Science* **351** 1061 (2016),

arXiv:1509.05691.

[31] Y. Wang and P. Narang. "Anisotropic scattering in the goniopolar metal $NaSn_2As_2$", *Physical Review B* **102** 12 (2020).

[32] A. A. Zibrov *et al.* "Emergent Dirac gullies and gully-symmetry-breaking quantum Hall states in ABA trilayer graphene", *Physical Review Letters* **121** 16 (2018).

[33] N. W. Ashcroft and N. D. Mermin. *Solid-State Physics* (Brooks Cole, 1976).

[34] In a viscous Fermi liquid, the bulk viscosity $\zeta \sim (T/T_F)^4 \mu$ is strongly suppressed at low temperature relative to other viscosity components μ [48] and therefore often neglected. Additionally, in this work, we make approximations which lead to an incompressible fluid $v_i \approx \epsilon_{ij}\partial_j\psi$ and therefore remove ζ entirely from the dynamics of the fluid. However, from symmetry considerations alone, we nevertheless proposed a device which isolates the dissipative effects of ζ and could potentially thereby enable its measurement.

[35] S. A. Hartnoll. "Theory of universal incoherent metallic transport", *Nature Physics* **11** 54 (2015), arXiv:1405.3651.

[36] This occurs due to the peculiar mixing of ideal and dissipative hydrodynamic coefficients in the momentum equation. For time-dependent phenomena, the incoherent conductivity can qualitatively modify hydrodynamics [49, 50].

[37] $I(s) = \pm I_0 \mathrm{rect}\left[(s \pm d/2)/a\right]$, where $\mathrm{rect}(x)$ is defined to be 1 for $|x| \leq 1/2$, and 0 otherwise.

[38] W-K. Tung. *Group Theory in Physics*, (World Scientific, 1985).

[39] In principle there is also a dissipative contribution $W_{\mathrm{inc}} = D\chi^{-1}(\nabla\rho)^2$, with χ the charge susceptibility, due to incoherent currents in the fluid [1], but this contribution is negligible due to the hydrodynamic approximations that lead to Eq. (3). In any case, since the gradient $\nabla\rho$ transforms under D_8 as a vector, this term (like the ohmic heating) cannot even in principle generate *center* heat in the dihedral viscometer unless it is in the R_1 configuration.

[40] J. Zhang *et al.* "Anomalous thermal diffusivity in underdoped $YBa_2Cu_3O_{6+x}$", *Proceedings of the National Academy of Sciences* **114** 21 (2017).

[41] P. Neumann *et al.* "High-Precision Nanoscale Temperature Sensing Using Single Defects in Diamond", *Nano Letters* **13** 6 (2013).

[42] G. Wagner. "Boundary conditions for electron flow in graphene in the hydrodynamic regime", arXiv:1509.07113.

[43] E. Kiselev and J. Schmalian. "Boundary conditions of viscous electron flow", *Physical Review B* **99** 3 (2019), arXiv:1806.03933.

[44] R. Moessner, P. Surówka N. Morales-Durán, and P. Witkowski. "Boundary-condition and geometry engineering in electronic hydrodynamics", *Physical Review B* **100** 15 (2019), arXiv:1903.08037.

[45] P. Rao and B. Bradlyn. "Hall viscosity in quantum systems with discrete symmetry: point group and lattice anisotropy", *Physical Review* **X10** (2020).

[46] I. S. Burmistrov *et al.* "Dissipative and Hall Viscosity of a Disordered 2D Electron Gas", *Physical Review Letters* **123** 2 (2019).

[47] J. M. Epstein and K. K. Mandadapu. "Time-reversal symmetry breaking in two-dimensional nonequilibrium viscous fluids", *Physical Review E* **101** 5 (2020).

[48] J. Sykes and G. A. Brooker. "The transport coefficients of a Fermi liquid", *Annals of Physics* **56** 1 (1970).

[49] A. Lucas. "Sound waves and resonances in electron-hole plasma", *Physical Review* **B93** 245153 (2016), arXiv:1604.03955.

[50] A. Lucas and S. Das Sarma. "Electronic sound modes and plasmons in hydrodynamic two-dimensional metals", *Physical Review* **B97** 115449 (2018), arXiv:1801.01495.

[51] A. Lucas and S. A. Hartnoll. "Kinetic theory of transport for inhomogeneous electron fluids", arXiv:1706.04621.

[52] A. Lucas. "Stokes paradox in electronic Fermi liquids", *Physical Review* **B95** 115425 (2017), arXiv:1612.00856.

[53] M. Qi and A. Lucas. "Distinguishing viscous, ballistic, and diffusive current flows in anisotropic metals", arXiv:2107.01216 (2021).